JPNT 4(1), 1-7 (2015)
http://dx.doi.org/10.11003/JPNT.2015.4.1.001

JPNT Journal of Positioning, Navigation, and Timing

GNSS Airborne Multipath Error Modeling Under UAV Platform and Operating Environment

Minchan Kim, Kiwan Kim, Dong-Kyeong Lee, Jiyun Lee†
Department of Aerospace Engineering, Korea Advanced Institute of Science and Technology, Daejeon 305-701, Korea

ABSTRACT

In the case of an unmanned aerial vehicle (UAV) equipped with a GNSS sensor, a boundary line where the vehicle can actually exist can be calculated using a navigation error model, and safe navigation (e.g., precise landing and collision prevention) can be supported based on this boundary line. Therefore, for the safe operation of UAV, a model for the position error of UAV needs to be established in advance. In this study, the multipath error of a GNSS sensor installed at UAV was modeled through a flight test, and this was analyzed and compared with the error model of an existing manned aircraft. The flight test was conducted based on a scenario in which UAV performs hovering at an altitude of 40 m, and it was found that the multipath error value was well bound by the error model of an existing manned aircraft. This result indicates that the error model of an existing manned aircraft can be used in operation environments similar to the scenario for the flight test. Also, in this study, a scenario for the operation of multiple UAVs was considered, and the correlation between the multipath errors of the UAVs was analyzed. The result of the analysis showed that the correlation between the multipath errors of the UAVs was not large, indicating that the multipath errors of the UAVs cannot be canceled out.

Keywords: GNSS, multipath, UAV flight test, error modeling

1. INTRODUCTION

Based on the successful application cases of a military unmanned aerial vehicle (UAV), developed countries have introduced the application of UAV into the public sector, and it has also been used in the civilian sector in various forms. UAV has thus far been used in limited fields such as crop situation survey, smuggling surveillance, broadcasting and communication repeater, and meteorological observation. However, the possibility and range of the commercial use of UAV have rapidly expanded as shown by the fact that foreign popular enterprises (e.g., Amazon and Google) recently announced plans to actively use UAV for product shipping (CBS News 2013, New York Times 2014). As the operation of commercial UAV has gradually increased and the missions have gradually been automated, accurate and safe navigation of UAV for successful mission performance and safe return is more important than ever.

A navigation sensor that is commonly used for aircraft is a Global Navigation Satellite System (GNSS) sensor. It has a lot of advantages such as global position estimation and curved approach, and thus has replaced the ground-based navigation systems of an existing manned aircraft such as Instrument Landing System (ILS) and Microwave Landing System (MLS). A GNSS sensor receives signals transmitted from satellites that are far away from the Earth, and thus has a number of errors. Therefore, for an existing manned aircraft, a boundary line where the vehicle can actually exist at a high probability ($1\text{-}10^{-7}$~$1\text{-}10^{-9}$) is defined by establishing an error model of GNSS, and safe navigation is supported based on this (RTCA SC-159 2004). In the operation of UAV for civilian purposes, use of a GNSS sensor is also expected. Accordingly, the safety of navigation information should be guaranteed by examining UAV-specific GNSS sensor errors and by establishing an error model that is appropriate for the characteristics of the corresponding elements, similar to an existing manned aircraft. If the position error of UAV is accurately modeled, a boundary line where the vehicle can

Received Dec 11, 2014 **Revised** Feb 09, 2015 **Accepted** Feb 09, 2015
†**Corresponding Author**
E-mail: jiyunlee@kaist.ac.kr
Tel: +82-42-350-3725 Fax: +82-42-350-5765

http://www.gnss.or.kr Print ISSN: 2288-8187 Online ISSN: 2289-0866

actually exist can be defined based on the modeled error, and precise and safe navigation (e.g., precise takeoff and landing and the prevention of collision between UAVs) can be performed based on this.

The GNSS error of UAV consists of the residual tropospheric delay error (σ_{tropo}), the residual ionospheric delay error (σ_{iono}), and the error from the receiver installed at the aircraft (σ_{air}) (Misra & Enge 2001). In this regard, σ_{air} can be divided into the receiver noise error of the vehicle (σ_{noise}) and the multipath error ($\sigma_{multipath}$). For the tropospheric delay error and the ionospheric delay error, errors are introduced to manned and unmanned aerial vehicles through the same process regardless of the types of the vehicles. Therefore, for these error elements, the error of UAV can be estimated using the error model for an existing manned aircraft. Also, the receiver noise error constituting σ_{air} changes depending on the type of the receiver, and an existing established receiver error model can be used depending on the type of the receiver installed at manned and unmanned aerial vehicles. However, the multipath error occurs due to the reflection or scattering of GNSS signals by obstacles, and is affected by the local environmental factors of the surrounding area. Although an antenna and a receiver with the same performance are used, it is difficult to utilize the multipath error model of an existing manned aircraft as it stands, because UAV has a body shape that is different from that of a manned aircraft and is operated at a lower altitude. Therefore, a multipath error model that is appropriate for the operation characteristics of UAV needs to be re-established. For this purpose, in this study, the multipath error of UAV ($\sigma_{multipath}$) was estimated and modeled by collecting GNSS signals through a UAV flight test, and this was verified through comparison with the error model of an existing manned aircraft. In Section 2 of this paper, an algorithm for estimating a multipath error using the GNSS data collected through an experiment was explained; and in Section 3, the test site for the flight test and the flight platform were explained in detail. In Section 4, a UAV multipath error model based on the flight test was suggested, and the correlation between the multipath errors of UAVs was analyzed.

2. METHODOLOGY FOR AIRBORNE MULTIPATH MODELING

A multipath error occurs due to the reflection or scattering of GNSS signals by obstacles, and thus is basically affected by the shape of a body. The effect of the reflected signals is determined by antenna gain and the correlator

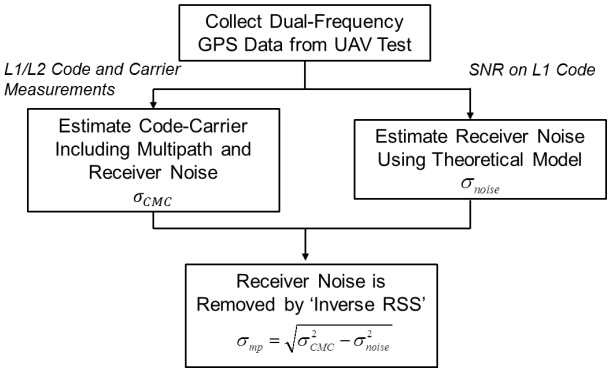

Fig. 1. Data analysis process of airborn multipath estimation.

duration of a receiver. Also, the multipath error of code measurement decreases during a code-carrier smoothing filter process, and thus the time constant of the filter has a large effect on the multipath error. UAV has a body shape that is different from that of a manned aircraft, and thus signals reflected by the bodies are different. Depending on the assigned mission, UAV can be operated at a lower altitude than a manned aircraft, and thus signals reflected from the ground surface or buildings on the ground could be received. Therefore, althou gh an antenna and a receiver that are identical to those of a manned aircraft are used, the multipath error of UAV should be modeled based on experiment data. This study aimed to model a multipath error due to the body shape of UAV and the flight environment, rather than receiver and antenna characteristics. For this purpose, dual-frequency GNSS data were collected through a UAV flight test, and a multipath error was estimated based on this. Fig. 1 shows the data analysis process for the estimation of a multipath error.

Based on the dual-frequency GPS data collected by UAV, Code Minus Carrier (CMC) estimates can be calculated using the code measurement and carrier measurement of the L1 frequency (ρ_{L1}, ϕ_{L1}) as shown in Eq. (1).

$$\rho_{L1} - \phi_{L1} = 2I + M_{L1} - m_{L1} - \lambda_1 N_{L1} + \varepsilon_{\rho 1} + \varepsilon_{\phi 1} \qquad (1)$$

CMC estimates include the ionospheric delay error I, the code and carrier multipath errors (M_{L1} and m_{L1}), the receiver noises of code and carrier measurements ($\varepsilon_{\rho 1}$ and $\varepsilon_{\phi 1}$), and the integer ambiguity of carrier measurement ($\lambda_1 N_{L1}$). In this equation, the multipath error and receiver noise of carrier measurement are sufficiently smaller than those of code measurement, and thus can be ignored. Also, integer ambiguity does not change in a section where a cycle slip does not occur, and thus $\lambda_1 N_{L1}$ can be regarded as a bias. Therefore, the sum of the multipath error and receiver noise of code can be expressed as Eq. (2).

http://dx.doi.org/10.11003/JPNT.2015.4.1.001

$$\rho_{L1} - \phi_{L1} - 2I - bias = M_{L1} + \varepsilon_{\rho 1} \tag{2}$$

Using dual-frequency carrier measurement, ionospheric delay can be estimated as shown in Eq. (3). In this equation, if it is also assumed that a cycle slip does not occur, the term $\frac{\lambda_1 N_{L1} - \lambda_2 N_{L2}}{\gamma - 1}$ which includes integer ambiguity does not change, and thus this term can be expressed as a bias.

$$\frac{\phi_{L1} - \phi_{L2}}{\gamma - 1} = I + \frac{\lambda_1 N_{L1} - \lambda_2 N_{L2}}{\gamma - 1} = I + bias \tag{3}$$

When the value I in Eq. (3) is substituted into Eq. (2), the sum of the multipath error and receiver noise of code measurement can be calculated as shown in Eq. (4). The bias in Eq. (4) can be eliminated by subtracting the average value of measurement from the measurement calculated using Eq. (4).

$$\rho_{L1} - \phi_{L1} - 2\left(\frac{\phi_{L1} - \phi_{L2}}{\gamma - 1}\right) = M_{L1} + \varepsilon_{\rho 1} + bias \tag{4}$$

The standard deviation of the measurement calculated by Eq. (4) (σ_{CMC}) represents the standard deviation value of the sum of multipath error and receiver noise. In this study, only the multipath error term was estimated by eliminating receiver noise through 'inverse Root Sum Square' as shown in Eq. (5), assuming that multipath error and receiver noise are independent.

$$\sigma_{mp} = \sqrt{{\sigma_{CMC}}^2 - {\sigma_{noise}}^2} \tag{5}$$

The standard deviation of receiver noise was calculated using the theoretical model shown in Eq. (6), and this was removed from the CMC estimation value (McGraw et al. 2000).

$$\sigma_{noise} = \lambda_c \sqrt{\frac{d}{8C/N_0 \tau}} \tag{6}$$

where λ_c is the wavelength of the code chip (in meters), d is the correlate spacing, C/N_0 is the carrier to noise value in units of ratio-Hz, and τ is the smoothing time constant.

3. FLIGHT TEST CONFIGURATION

Fig. 2 shows the UAV flight test site for the collection of multipath errors. For UAV that is to be operated in the civilian sector in the future, it would be inevitable that UAV is affected by buildings and trees that could block GNSS signals or could induce multipath errors. Thus, the flight test site was selected to be an empty lot on the western side of the Industrial Engineering and Management Building in KAIST considering the environment for future UAV operation. As shown in the figure, buildings were located and many trees were distributed around the test site. For this reason, it was thought to be an appropriate site for collecting the multipath error of UAV that is to be operated in the civilian sector, and the flight test was performed based on a flight at a 40 m altitude.

Fig. 2. UAV flight test site at KAIST.

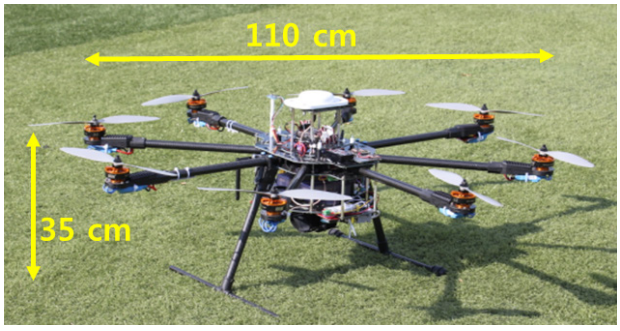

Fig. 3. Multi-copter UAV platform for flight test.

Figs. 3 and 4 show the flight platform for performing the flight test. An octocopter with a 110 cm diameter and a 35 cm height was used, and high-performance NovAtel FlexPak-6 receiver and NovAtel ANT-A72GOLA-TW antenna were used to collect dual-frequency GPS data. Also, a data logger and an APM 2.6 controller using the PID feedback control technique were installed. This octocopter performs flight using the navigation solution of the FlexPak-6 receiver, and records the GNSS data of the FlexPak-6 receiver in the data logger at the same time.

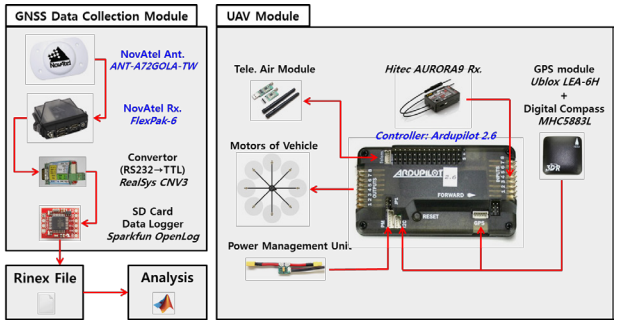

Fig. 4. GNSS data collection module and UAV control module for flight test.

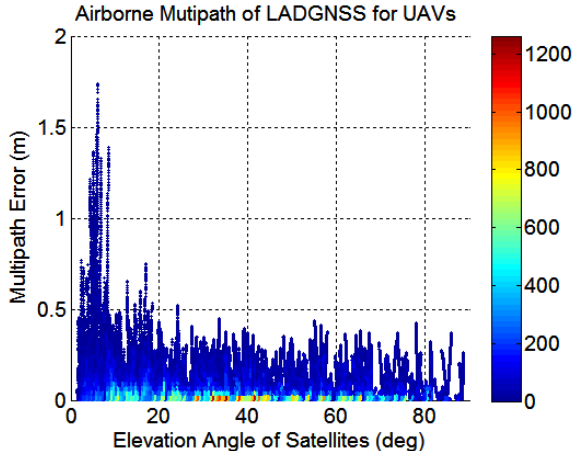

Fig. 5. UAV multipath colleted from UAV flight test.

4. RESULTS

4.1 Multipath Error Model of UAV

The UAV flight test for the collection of multipath errors was conducted based on a scenario in which the UAV performs hovering at an altitude of 40 m, and a total of 49 test flights were carried out. In each flight test, the UAV performed hovering on a spot of the site shown in Fig. 2 at a constant height. The location changed in each test within the boundary shown in Fig. 2 (about a 30 m radius), but the altitude was maintained at 40 m. This corresponded to a flight time of a total of 4 hours and 3 minutes. Dual-frequency GNSS data were collected through the NovAtel receiver using the 0.1 chip C/A code correlator installed at the UAV, and the multipath error was calculated based on the algorithm explained in Section 3. The UAV flight test was performed at an altitude that is much lower than the flight altitude of a manned aircraft. As a result, it would include a lot of effects of signals reflected from the ground as well as signals reflected from the body. The multipath error was calculated for each satellite observed during about 4 hours of flight test. Therefore, a maximum of 4-hour data could be obtained for each satellite, and the total sum of the multipath error data of all the observed satellites corresponded to 28 hours. Fig. 5 shows the multipath errors observed during the flight test depending on the elevation angle of the satellite. In Fig. 5, the x-axis represents the elevation angle of the satellite, y-axis represents the multipath error value, and the color bar on the right side represents the number of data for each 0.5deg*0.02m pixel. As shown in the graph, the multipath error value increased as the elevation angle decreased. This is the typical characteristic of a multipath error, and it is because signals are scattered or reflected by buildings, etc. as the elevation angle of the satellite decreases. The maximum multipath error (about 1.7 m) was observed at a satellite elevation angle of 6 degrees, and the multipath error decreased when the elevation angle was lower than 6 degrees. This is because when the elevation angle was lower than 6 degrees, the number of data was insufficient, and thus accurate characteristic of the multipath error could not be reflected.

The blue curved line in Fig. 6 shows the standard deviation value of the multipath error collected through the flight test, and this was calculated based on the bin size of the satellite elevation angle of 2 degrees. The red curved line in the graph shows the result of the Airframe Multipath Designator (AMD)-A standard airborne multipath model for manned aircraft suggested by RTCA (2004). This model was established using the actual flight data of a number of manned aircraft equipped with a receiver based on 100-second smoothing (Booth et al. 2000). This model can be expressed as a function of the elevation angle of the satellite (el) as shown in the following equation.

$$\sigma_{Std.multipath}(el) = 0.13 + 0.53e^{(-el/10^{\circ})} \quad (7)$$

The existing model is a multipath error model established using the data collected during flight without an obstacle (e.g., a nearby building). In the flight test of this study, the flight vehicle was higher than nearby buildings, and thus the multipath reflected from the aircraft body and the ground would have a larger effect than the multipath error due to the nearby buildings. As shown in the graph, the multipath error of the UAV obtained through the flight test was well bound by the standard airborne multipath model. This indicates that the existing model could be used to estimate multipath error values in the flight environment of the flight test (i.e., when UAV equipped with the 0.1 chip C/A code correlator and the receiver using 100-second smoothing performs hovering at an altitude higher than

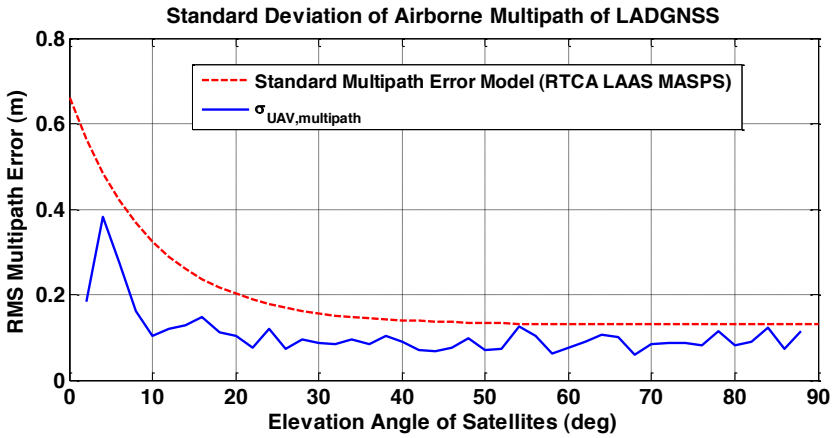

Fig. 6. Standard deviation of observed UAV multipath compared with standarad model.

nearby buildings on a site with a flat ground surface as in an airport). However, if there is direct effect of buildings as the nearby area is surrounded by the buildings, the existing model, which had been established in an environment without an obstacle, could not be used. The UAV used in the test is a flight vehicle that can be used for commercial purposes (e.g., unmanned parcel service), and it was analyzed only for a specific operation scenario. UAVs for commercial purposes have various sizes and types (e.g., fixed wing and rotor). Also, the antenna position, flight altitude, maneuver, and surrounding environment would have a large effect on the multipath error of UAV. Therefore, for the operation of UAV in the civilian sector, a multipath error model needs to be established for each operation scenario that is appropriate for an operation purpose. In the future, for the commercial operation of UAV (e.g., unmanned parcel service), a multipath error for each operation scenario will be established based on the octocopter by diversifying the flight altitude, surrounding environment, maneuver, etc.

4.2 Analysis of the Correlation Between the Multipath Errors of UAVs

When performing missions such as reconnaissance and surveillance, the mission can be more effectively performed if multiple UAVs in formation are used rather than a single UAV. During the simultaneous operation of multiple UAVs, an essential consideration is the prevention of collision between UAVs. As mentioned earlier, the safety of UAV can be increased by modeling the error of a GNSS sensor. In the earlier section, a multipath error among the GNSS sensor errors of a single UAV was analyzed, and the relevant error model was suggested. If a boundary line where a vehicle can actually exist is defined using this model, multiple UAVs can be operated so that the boundary line of each UAV is not intruded, thereby preventing a collision.

If the errors of UAVs in operation have similar directions and sizes, boundary lines can be defined by ignoring the correlated errors in terms of relative distance. When the width of the boundary line between UAVs narrows, the operation range of each UAV widens, and thus the efficiency of mission performance would increase. Therefore, a correlation analysis of the GNSS sensor error factor should be carried out to increase the operation efficiency of multiple UAVs. In this study, the analysis of the correlation between the multipath errors of two UAVs was performed. Two octocopters with the specification identical to the flight platform configuration for the UAV multipath error collection described earlier were made to hover at the same altitude (20 m from the ground), and the multipath errors were collected at the same time. In this regard, the horizontal distance between the two UAVs was maintained at 10 m. A total of 10 test flights were carried out, and this corresponded to a flight time of a total of 20 minutes. Fig. 7 shows the multipath errors of the PRN 05 and PRN 15 satellites collected by the two UAVs. The graph shows the result of one flight among the 10 flight tests. The x-axis represents the data collection period during the flight test, and the y-axis represents the multipath error. The average Pearson correlation coefficient between the multipath errors of all the satellites collected by the two UAVs was -0.12, indicating that there was almost no correlation between the two multipath errors.

UAV has a limited flight time, and it is difficult to collect long-term multipath errors using UAV. Therefore, to analyze the correlation between the multipath errors collected over a long period, multipath errors were collected by installing two antennas at the rooftop of the Mechanical Engineering Building in the campus of KAIST. The two installed

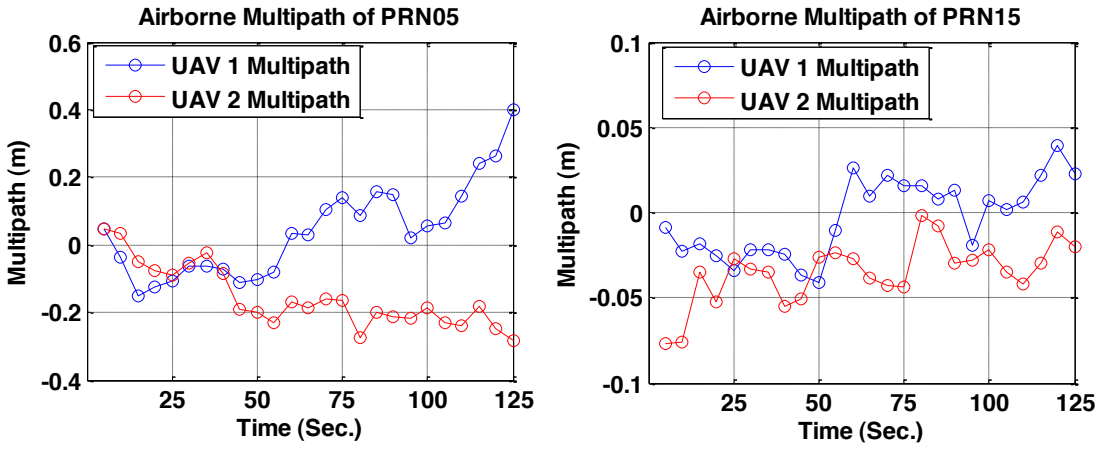

Fig. 7. Comparision of UAVs multiapth viewing PRN 05 and PRN 15.

antennas were 16 m away from each other. Fig. 8 shows the multipath errors of the PRN 05 satellite collected by the two antennas. The blue and red lines in the graph represent the multipath errors of each antenna. The elevation angles of the PRN 05 satellite observed at the two antennas changed similarly, and thus the sizes of the two errors depending on time also changed similarly. At both ends of the graph, the elevation angle was low and thus the multipath error was large; and at the center part, the elevation angle was relatively high (66°) and thus the multipath error was small. However, the Pearson correlation coefficient between the two errors was 0.21, indicating that there was almost no correlation. In other words, the maximum sizes of the two multipath errors depending on the elevation angle were similar, but the errors did not occur at the same time in the same size. The average Pearson correlation coefficient between the multipath errors of all the satellites collected in the test was 0.16, indicating that there was

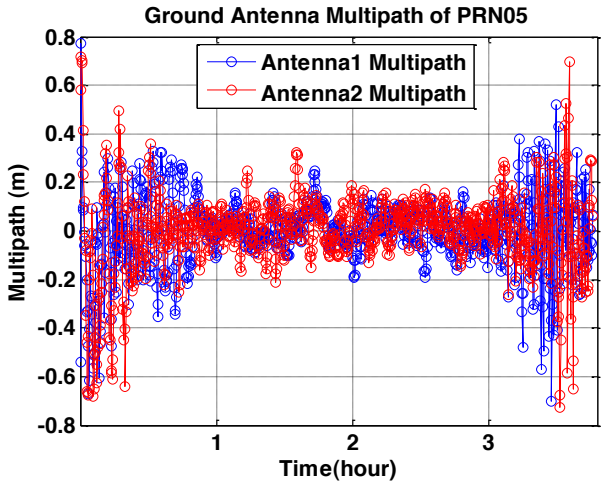

Fig. 8. Comparision of ground antennas multiapth viewing PRN 05.

almost no correlation between the multipath errors of the two antennas for all the satellites. This result suggests that the errors between the two antennas cannot be canceled out because the instantaneous multipath errors had no correlation even though the distance between the antennas was close (a few tens of meters).

5. CONCLUSIONS

In this study, the multipath error of GNSS signals in a UAV operation environment where a GNSS sensor is used as the navigation sensor was modeled through the flight test of UAV. UAV has a body shape that is different from that of a manned aircraft and can be operated at a relatively lower altitude depending on the mission. Therefore, an error model that is appropriate for the operation characteristics of UAV needs to be established. An accurate error model is essential for calculating a boundary line where a vehicle can actually exist, and this would enable the safe navigation of UAV. In this study, to collect the multipath error of UAV, a flight test was carried out based on a scenario in which UAV performs hovering at an altitude of 40 m. The results of the test indicated that the multipath error of the UAV increased as the elevation angle of the satellite decreased, and the value did not exceed the error model of an existing manned aircraft. This indicates that the AMD-A standard airborne multipath model for manned aircraft could be used to estimate the multipath error of UAV in an operation environment similar to the test scenario where UAV performs hovering at an altitude higher than nearby buildings on a site with a flat ground surface as in an airport using a 0.1 chip C/A code correlator and a receiver based on 100-second smoothing. However, this result is not applied

to every case of UAV operation. If there is direct effect of buildings as the nearby area is surrounded by the buildings, the existing established model could not be used. Therefore, in the future, a multipath error analysis will be performed considering various flight platforms, flight environments and altitudes for UAV operation. Also, in this study, a scenario for the operation of multiple UAVs was considered, and the correlation between the multipath errors of the UAVs was analyzed. The results of the analysis indicated that the errors between the UAVs cannot be canceled out because the multipath errors had almost no correlation even though the distance between the UAVs was close (a few tens of meters).

With the expansion of the UAV application field, the type, flight altitude, and operation environment of UAV have been diversified. Therefore, for the operation of UAV in the civilian sector, a navigation error model that is appropriate for each operation scenario needs to be established. In this study, only the multipath error of a specific operation scenario was modeled; but in the future, the multipath errors of various UAV operation scenarios will be modeled based on the result of the flight test performed in this study. The error model of UAV established in this study could be used to calculate a boundary line where a vehicle can actually exist, and thus would be applied to various systems that utilize this safe distance such as precise navigation, automatic landing, and maintaining a separation distance between UAVs.

ACKNOWLEDGMENTS

Minchan Kim was supported by the Agency for Defense Development under the contract UE124026JD. Kiwan Kim was supported by the KAIST Institute.

REFERENCES

Booth, J., Murphy, T., Clark, B., & Liu, F. 2000, Validation of the Airframe MultipathError Allocation for Local Area Differential GPS, Proceeding of the IAIN/ION Meeting, San Diego, CA, 26-28 June 2000.

CBS News 2013, Amazon Unveils Futuristic Plan: Delivery by Drone, 1 Dec 2013, http://www.cbsnews.com/news/amazon-unveils-futuristic-plan-delivery-by-drone/

McGraw, G. A., Murphy, T., Brenner, M., Pullen, S., & Dierendonck, A. J. V. 2000, Development of the LAAS Accuracy Models, Proceedings of ION GPS 2000, Salt Lake City, UT, 19-22 Sep 2000.

Misra, P. & Enge, P. 2001, Global Positioning System: Signals, Measurements, and Performance (Lincoln, MA: Ganga-Jamuna Press), pp.1-569

New York Times 2014, Google Joins Amazon in Dreams of Drone Delivery, 28 Aug 2014, http://bits.blogs.nytimes.com/2014/08/28/google-joins-amazon-in-dreams-of-drone-delivery/?module=Search&mabReward=relbias%3Ar%2C%7B%222%22%3A%22RI%3A17%22%7D

RTCA SC-159 2004, Minimum Aviation system Performance Standards for the Local Area Augmentation Systems, RTCA/DO-245A, Dec 2004.

Minchan Kim received his B.S. degrees in Aerospace Engineering form Korea Aerospace University, Koyang, Korea, in 2011. He is a Ph.D student in Aerospace Engineering at Korea Advanced Institute of Science and Technology. His current research mainly focuses on GNSS-based navigation system including GBAS.

Kiwan Kim received his B.S. degree in Aerospace Engineering form Korea Aerospace University (2013) and M.S. degree in Space Exploration Engineering form Korea Aerospace University (2015). His current research mainly focuses on GNSS-based navigation system for UAV.

Dong-Kyeong Lee received his B.S. in Aerospace Engineering from Korea Advanced Institute of Science and Technology (KAIST) in 2014. He is currently a M.S. student in the Department of Aerospace Engineering at KAIST. His research interests include GNSS augmentation system and UAV navigation system.

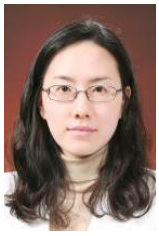

Jiyun Lee is an Associate Professor in the school of Mechanical Aerospace and Systems Engineering at Korea Advanced Institute of Science and Technology. She has supported the GBAS and SBAS program over the past eight years as a consulting professor at Stanford University and a Principal GPS Systems Engineer at Tetra Tech AMT. She received her B.S. degree from Yonsei University, M.S. degree from the University of Colorado at Boulder, and her Ph.D. from Stanford University (2005) in aeronautics and astronautics. Prior to joining AMT, she worked for SiRF Technology, Inc. as a Senior GPS systems engineer.